MONITORING ROCK GLACIER DYNAMICS IN THE HOHE TAUERN MOUNTAINS: INSIGHT INTO RECENT ALPINE PERMAFROST CHANGES

DOI:
UDC: 551.343.4-047.36:551.345(436)

Harald Zandler
Andreas Kellerer-Pirklbauer
Wolfgang Sulzer
University of Graz, Department of Geography and Regional Science, **Austria**

ABSTRACT

Changes in mountain permafrost are of major scientific and societal interest due to associated potential risks to mountain communities. Rock glaciers, which are slowly creeping debris-ice landforms typical of mountainous permafrost regions, are key indicators of permafrost dynamics. Their movement serves as a critical parameter for the Essential Climate Variable (ECV) permafrost. This study investigates the movement of two rock glaciers in the Hohe Tauern Mountain Range, Austria: Tschadinhorn rock glacier (TRG) and Leibnitzkopf rock glacier (LRG), during 2023–2024 and compares derived movement rates to previous rock glacier velocity studies of these sites, as well as to ground and air temperature records. For rock glacier velocity quantification, we used unoccupied aerial vehicles (UAVs) with real-time-kinematic capabilities to create geodatasets of high spatial resolution and accuracy for both years. Rock glacier movement patterns were calculated using orthoimages, aligned to an existing geodetic network, using a state-of-the-art image correlation algorithm (GeoCosiCorr3D).

Results show that TRG exhibited the highest published, photogrammetrically derived mean RGV to date, 3.8 m/year in 2023–2024, exceeding previous maxima of interpolated point measurements reported for 2014–2015 and photogrammetric data from 2015–2016. At LRG, the maximum velocity reached 6.2 m/year, surpassing the previously published maximum of 5.8 m/year, but with a spatial shift in the location of peak movement. Spatial patterns at LRG indicate deceleration within central sectors and acceleration at the frontal zone, whereas TRG shows a more uniform acceleration. The climate context supports these trends: long-term, regional station data registered an all-time annual temperature record in 2024, consistent with a positive temperature-RGV relationship. However, local ground and air temperature observations since 2018 reveal site-specific responses with no clear trends, but a tendency of higher movement rates in warmer years at TRG and no simple, uniform linkage at LRG, suggesting modulation by internal kinematics and spatial heterogeneities.

Our findings provide robust, spatially resolved velocity evaluations for two representative alpine rock glaciers in the Alps and demonstrate recent acceleration consistent with long-term ongoing warming. The results underscore the need for sustained, multi-sensor monitoring to disentangle climatic forcing from internal deformation processes, thereby improving process understanding and risk assessment in high-mountain permafrost environments.

Keywords: Permafrost, rock glacier velocity, UAV, climate change, Alps

INTRODUCTION

Global warming has profound impacts on mountain environments, driving widespread permafrost degradation and, as a direct consequence, increasing alpine geohazards [1]. Rock glaciers (RGs), widely distributed permafrost landforms in high-mountain systems, serve as key geo-indicators for the state of alpine permafrost and for past, present and projected climate change [2–4]. Monitoring RGs is therefore essential for understanding ongoing transformations in high mountain environments. A central parameter for evaluating permafrost conditions in RGs is their deformation and displacement, which has led to the recognition of rock glacier velocity (RGV) as an Essential Climate Variable (ECV) for permafrost[2,5]. Recent studies have documented an acceleration in RG movement driven by climatic forcing [2,4]. Therefore, continued research and sustained monitoring of RGV are critical for detecting, attributing, and predicting the effects of environmental change in alpine settings.

Due to its importance, surface velocities of RGs have been measured since the last century using both ground-based and remote sensing approaches. Ground-based methods, such as Differential Global Navigation Satellite System (DGNSS) surveys, provide precise point-based displacement measurements, while remote sensing techniques, including satellite imagery and Unoccupied Aerial Vehicle (UAV) photogrammetry paired with various surface velocity algorithms [6], enable spatially comprehensive assessments of surface deformations [7]. UAV-based approaches, in particular, offer high-resolution mapping of surface displacements, facilitating the analysis of spatial variability across the landform, and supporting standardized, multi-temporal comparisons.

To provide new insights into recent alpine permafrost dynamics, this study investigates the movement patterns of the two rock glaciers Tschadinhorn (TRG) and Leibnitzkopf (LRG) using UAV surveys. These two RGs are well suited for examining changes in permafrost behavior as their historical flow velocities have been intensively studied [8–10], they are located in close proximity to each other (~7 km) and are subject to similar regional topoclimatic and geological settings, and both are highly active. By comparing our UAV-derived velocity fields to existing remote sensing studies and regional climate data, we aim to interpret observed dynamics to assess regional similarities and differences.

STUDY AREA

Both RGs are located in the Schober Mountains, Hohe Tauern Mountain Range, in the political district of Lienz, Eastern Tirol, Austria (Figure 1). Elevations of the lower limit of these landforms are around 2640 m.a.s.l. for TRG and 2500 m.a.s.l for LRG. Geologically, both RGs are formed by metamorphic rock types, TRG by amphibolite and LRG by mica schist [4]. Detailed descriptions of both rock glaciers and their morphology can be found in the literature [8–10].

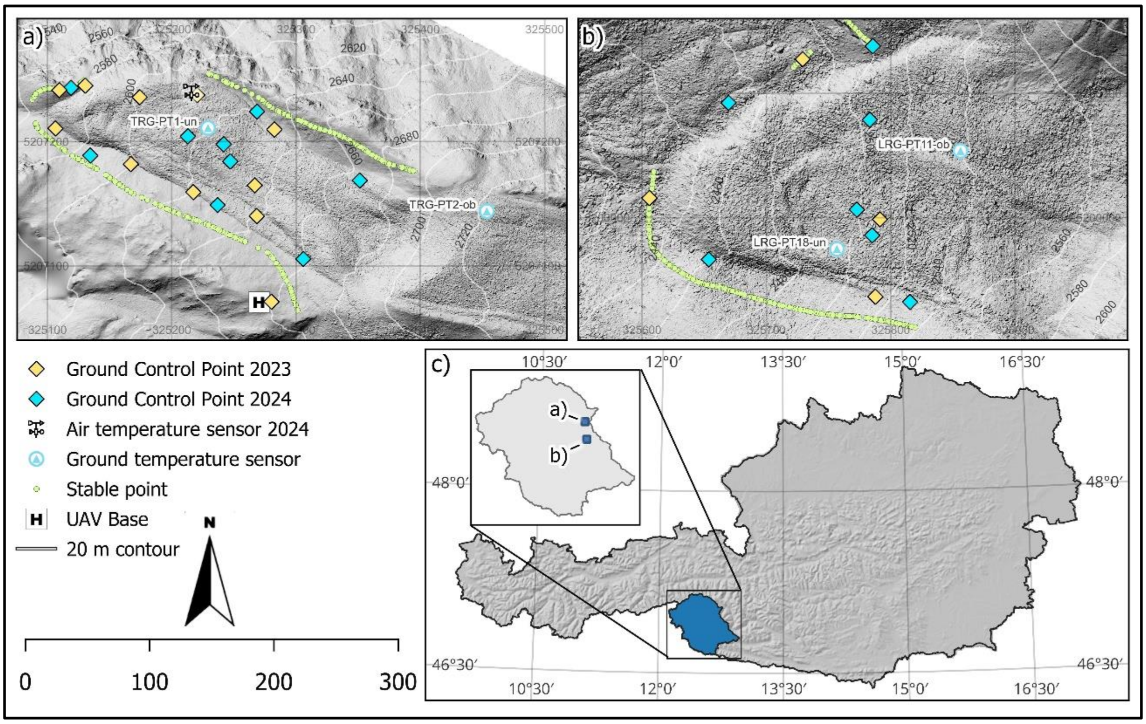

Figure 1: Overview of the studied rock glaciers TRG (a) and LRG (b) in 2024. Both rock glaciers are located in the political district of Lienz, Eastern Tirol, Austria, which is shown as blue polygon in (c). Coordinate reference system is 25833 (a, b) and 3416 (c). The UAV Base at the Leibnitzkopf research area is located approximately 200 m to the west outside of the map and was not covered by the UAV imagery. DEM data source for (c): [11]

DATA AND METHODS

We performed image acquisitions in August 2023 and 2024 at both sites using the UAV DJI Matrice 300 RTK, equipped with the photogrammetric camera DJI Zenmuse P1 with a focal length of 35 mm (Table 1). We used coordinates of an existing geodetic network, established by Viktor Kaufmann [8,10], and set up base stations at coordinates of respective fixed points for real-time-kinematic (RTK) corrections for terrestrial and UAV based DGNSS measurements. To assure high-accuracy, all images were recorded in RTK mode and post processed (Post-Processing Kinematic – PPK) using the local base station corrections and UAV DGNSS logs from the flights using the software Emlid Studio 1.9 [12]. This allowed for recording cm-accurate UAV images across all our research areas.

Table 1: Overview of UAV survey flight parameters at the two studied RGs

Location	Date [YYYY.MM.DD]	Ground sampling distance [m]	Number of images [n]	Ground control points [n]
TRG	2023.08.24	0.015	399	10
TRG	2024.08.29	0.015	601	7
LRG	2023.08.25	0.015	465	4
LRG	2024.08.30	0.015	587	7

Terrestrial DGNSS measurements of Ground Control Points (GCPs), colored targets that were placed previous to the flight, were performed using a base-rover configuration with an Emlid Reach RS2 and an Emlid Reach RS3 DGNSS [13]. Each target was measured three times to reduce measurement uncertainties with a ten second averaging interval each, and afterwards summarized to one mean coordinate for each GCP. Respective measurements served for checking the accuracy of the photogrammetric products and were not used in the processing or bundle block adjustment. Due to changing weather conditions and therefore, temporal resources, as well as unstable and difficult terrain, the number of GCPs varied between the different surveys (Table 1).

Photogrammetric processing, including image alignment, bundle adjustment, creation of point clouds, digital surface models and orthoimages, was performed using a standard Structure-from-Motion (SfM) approach in Agisoft Metashape 2.2 [14]. Afterwards, we resampled the resulting, coregistered orthoimages to achieve an exact match of the different time periods and to derive the desired resolution for computing surface displacement and velocity. In this study, we aim to derive horizontal (2D) surface displacement, as this variable is comparable to existing research at both sites. Various algorithms for the calculation of surface displacement exist [6]. For regular displacements, intensity tracking methods using cross-correlation are considered as a suitable approach [7]. The approach uses rectangular sliding windows to correlate sections of base- with areas of target images, representing different acquisition times, and derives displacement from the shift of highest-correlating windows. We applied the python based geoCosiCorr3D algorithm [15,16], an improvement of the methodology of Leprince et al. [17], which uses a normalized cross-correlation method of fast fourier-transformed, multi-scale sliding windows, as it showed good performance in comparison to other approaches in situations of horizontal deformations [18,19]. For the algorithm, several parameters have to be defined. The most important parameter is the window size, as it sets the area for the correlation window, but also depends on the maximum expected displacement. Existing studies recommend a window size that is about two times the displacement to be measured [17]. Therefore, the window size in pixels depends on the resolution of the input rasters and the maximally expected displacement. We selected two different parameterizations: a) parameters similar to existing research for both sites, which used an input raster resolution of 0.2 m, a window size of 31 pixels and an output grid spacing of 5 m [9,10], whereby we increased the window size to 64 pixels to match recommendations for the applied frequency algorithm [17] and b) a higher resolution version using 0.03 m input rasters, a window size of 512 and an output grid spacing of 0.06 m (Table 2).

Table 2. Overview of parametrization for velocity computations at both studied RGs.

Location	Input resolution [m]	Output grid spacing [m]	Window size [pixels]	Abbreviation
TRG	0.2	5.00	64	TH_020m_64
TRG	0.03	0.06	512	TH_003m_512
LRG	0.2	5.00	64	LK_020m_64
LRG	0.03	0.06	512	LK_003m_512

Both parameterizations were calculated with the red band only as this approach showed good performance at velocity computations in high-mountain settings and lower atmospheric scattering effects are expected [20].

To evaluate the velocity computations and the detection threshold for displacements, we mapped areas outside of the RG that represent potentially stable terrain with an expected displacement of zero, as this approach is frequently used in permafrost research and easily comparable [21]. Therefore, we mapped polylines in (potentially) stable terrain, and calculated 200 random points along the lines with a minimum distance of 1 m around each RG (Figure 1). Computed velocities from the different approaches were subsequently extracted and used to calculate the level of detection (LoD) in m/year according to Fey and Krainer [7] as:

$$LoD = (\mu + 2 * \sigma)$$

Thereby, μ represents the mean displacement on stable points in m/year and σ is the standard deviation of displacements at stable points in m/year.
Comparison to existing results is conducted by using areal averages of clearly defined Areas Of Interest (AOI), as outlined in Kaufmann et al. 2018 [8] in case of TRG, or the maximum displacement in addition to newly mapped AOIs around geodetic survey points used in Kaufmann et al. [10], due to the unavailability of existing reference areas.
Own air and ground temperature measurements were conducted between 2018 and 2024 using miniature temperature dataloggers. The dataloggers used are products from GeoPrecision, whereby each data logger is equipped with a PT1000 temperature sensor and records hourly temperature values. The loggers have an accuracy of ±0.05 °C, a range of −40 to +100 °C and a calibration drift <0.01 °C yr−1. From these measurements, mean annual ground surface temperature (MAGST) and mean annual air temperature (MAAT) values have been calculated based on monthly averages from September to August of the following year. A snow cover day was considered as such when the weekly standard deviation of the mean daily ground surface temperature was ≤0.25 °C [22]. For long term climate data, we used the homogenized HISTALP dataset [23] for air temperature at the station Sonnblick (SON), as it is a high-mountain weather station (3105 m a.s.l.) and has a distance of less than 25 km to the studied RGs. We did not use the whole time series available, which starts in 1887, but used data from 1950 onwards, as the onset of published RGV analysis was 1954 at both sites [9,10]. We used Locally Weighted Scatterplot Smooth (LOWESS) to visualize smoothed non-linear trends, a widely used and comparable method [24], with a data fraction for smoothing of 25 years following recommendations in existing climate research [25]. For linear trends, we used Sen's slope together with Mann–Kendall significance testing for the trend direction, because Sen's slope is more robust compared to parametric methods and as Mann–Kendall is considered suitable for climatological datasets [26,27]. We did not calculate trends for our own climate measurements due to the short available time period.

RESULTS AND DISCUSSION

Photogrammetric processing of the UAV images resulted in independently assessed horizontal errors between 0.02 m to 0.04 m (Table 3). No clear pattern was visible regarding the X or Y domain of horizontal errors, but elevation errors (Z) were slightly higher than horizontal errors. Accumulation of errors for two periods would amount to 0.06 m at TRG and 0.05 m at LRG.

Table 3. Error measures of the UAV campaigns using independent GCPs

Region-Year	n	X [m]	Y [m]	Z [m]	XY [m]
TRG2023	10	0.020	0.011	0.042	0.022
TRG-2024	7	0.035	0.021	0.026	0.040
LRG-2023	4	0.019	0.010	0.032	0.021
LRG-2024	7	0.013	0.026	0.048	0.029

Results of the period 2023-2024 showed a mean RGV of 3.80 m/year (3.79 m/year) for the lower (higher) resolution parameterization at TRG and of 3.54 m/year (3.66 m/year) for the lower (higher) resolution parameterization at LRG (Table 4).

Table 4. Overview of mean RGV and LoD values with different parameterizations. All LoDs were calculated using 200 points

Parameterization	Mean RGV [m/year]	LoD [m/year]	Maximum displacement [m/year]
TRG_020m_64	3.80	0.029	4.66
TRG_003m_512	3.79	0.032	4.70
LRG_020m_64	3.54	0.069	6.19
LRG_003m_512	3.66	0.065	7.08

LoD values ranged from 0.03 m/year to 0.07 m/year, which is below 1% to 2% of the mean RGV. Maximum velocity values were at 4.66 m/year (4.70 m/year) at TRG and at 6.19 m/year (7.08 m/year) for the lower (higher) resolution parameterization at the LRG. TRG shows a zone with lower displacements in the southeast above a slope break, and a faster zone in the northwest including the tongue-shaped front, whereby lower velocities occur at the tongue of the RG and higher velocities in the middle of the southeastern part of this zone (Figure 2). The two parameterizations showed largely identical results. Maximum displacements were found in close proximity to maxima of existing studies. Decorrelations were visible at the slope break zone but not within the averaging area of the RG.

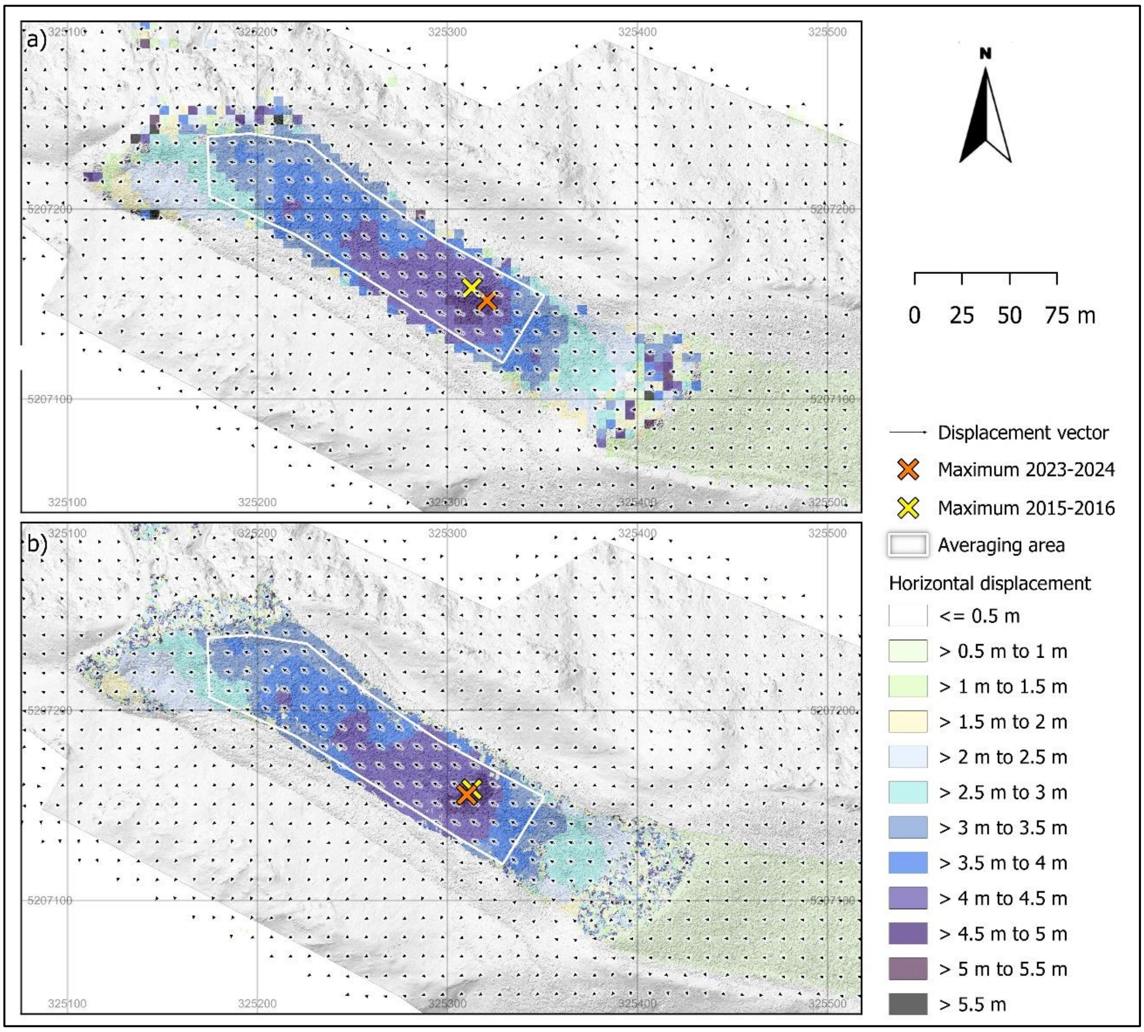

Figure 2. Derived displacements between 2023 and 2024 at the TRG with the parameterizations TRG_020m_64 (a) and TRG_003m_512 (b). Orange crosses mark the location of the maximum displacement of this study (4.66 m/year for TRG_020m_64 and 4.70 m/year for TRG_003m_512) compared to yellow crosses, indicating the approximate location of the maximum displacement (3.56 m/year) in 2015-2016 published in [8,9]. Displacement vectors are at map scale. White border shows the AOI for calculating mean RGV.

LRG showed high displacements of more than 4.5 m over a large area in the southwestern part and low velocities along a broad border zone in the northeast (Figure 3). Location of maximum values 2023-2024 were at different locations compared to previously published positions and were located at the southwestern end of the tongue. The different parametrizations largely showed similar results with some differences along the western tongue. A notable difference was decorrelation in the higher resolution parameterization north of the maximum value published in Kaufmann et al. [10].

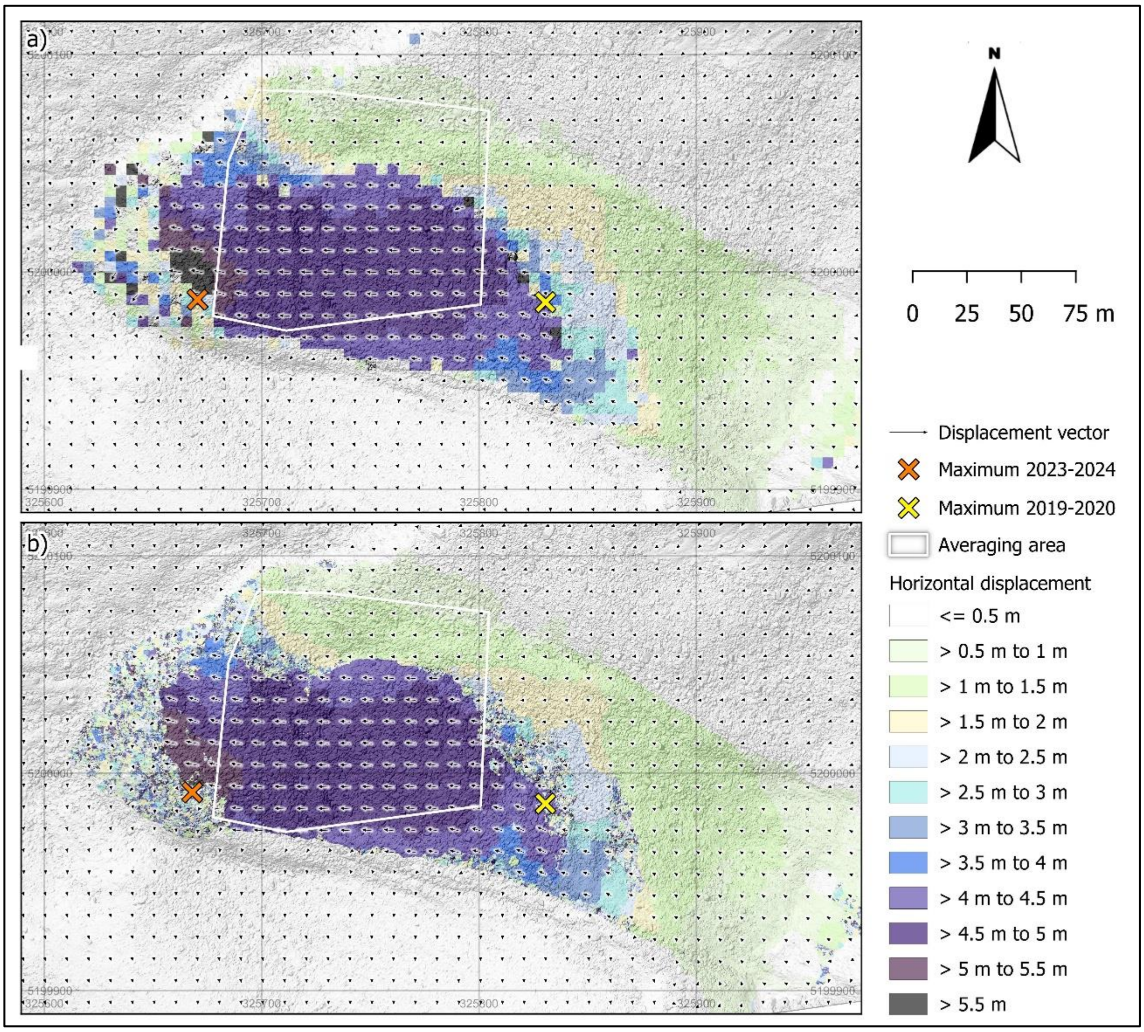

Figure 2. Derived displacements between 2023 and 2024 at the LRG with the parameterizations LRG_020m_64 (a) and LRG_003m_512 (b). Orange crosses mark the location of the maximum displacement of this study (6.2 m/year for LRG_020m_64 and 7.1 m/year for LRG_003m_512) compared to yellow crosses, indicating the approximate location of the maximum displacement (5.76 m/year) in 2019-2020 published in [10]. Displacement vectors are at map scale. White border shows the AOI for calculating mean RGV, which was mapped around geodetic survey points 2019 shown in Kaufmann et al. [10].

Long term climate data analysis shows an accelerating trend of increasing yearly temperatures with maximum mean values measured in 2024 (Figure 4). The 2023-2024 period of this study represents the warmest two-year period of the whole times series. On site weather stations show a similar pattern for MAGST and MAAT during 2018-2014 at TRG (Figure 5). Snow cover duration at TRG was the longest in 2023-2024 at the lower sensor and showed an intermediate duration at the upper sensor. The upper MAGST sensor values were among the highest at LRG, whereas the lower sensor showed the third lowest temperatures. Generally, both sites at LRG showed lower or similar temperatures compared to the 2019-2020 period. Snow cover duration was very low at both sensors at LRG compared to the whole time series and lower than the 2019-2020 values.

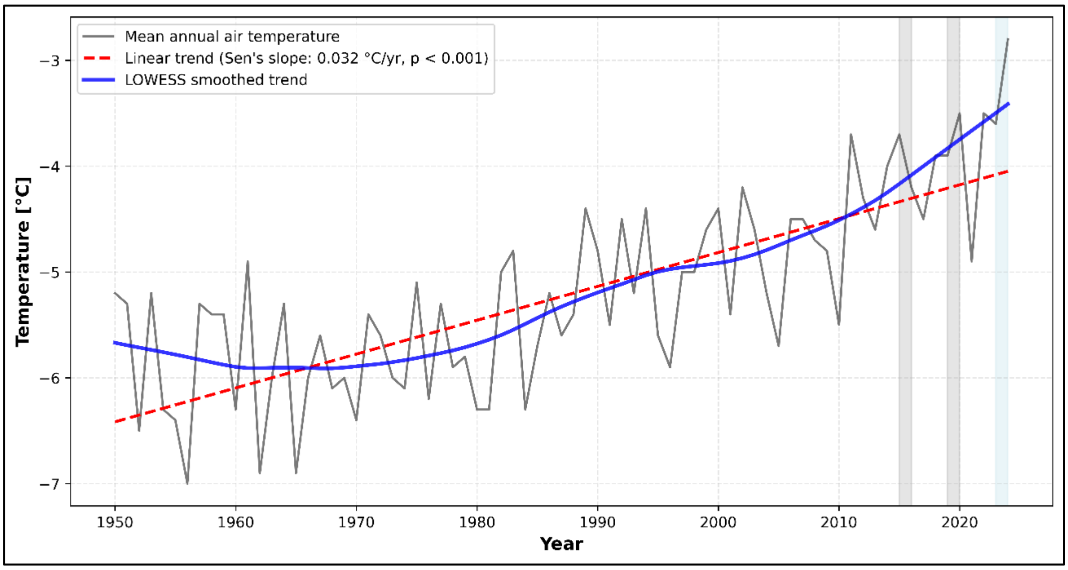

Figure 4. Mean annual temperatures and trends 1950-2024 at Sonnblick (3105 m a.s.l.). Grey bars indicate periods of published maximum values of existing photogrammetric research in 2015-2016 [8,9] at Tschadinhorn rock glacier and 2019-2020 at Leibnitzkopf rock glacier [10], and light blue bar indicates the period of the presented study. Data source: HISTALP 2026 [23]

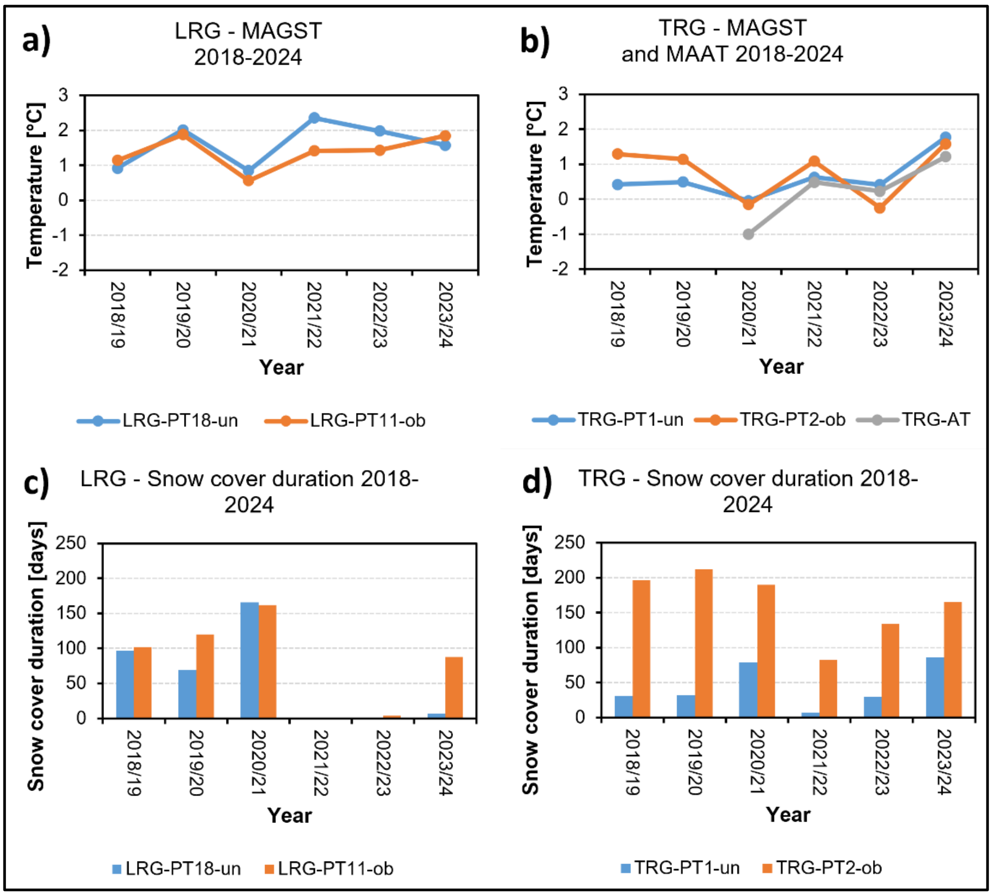

Figure 5. Temperature-derived parameters at the two rock glacier sites for the period 2018-2024: Mean annual ground surface temperatures (MAGST) and mean annual air temperatures (MAAT) for the LRG (a) and TRG (b) sites. Snow cover conditions were derived from the ground temperature data for the LRG (c) and TRG (d) sites. For location of sites refer to Figure 1

DISCUSSION

Our results indicate an increase of mean RGV at TRG compared to previously published values. The 2023-2024 mean was 3.80 m/year, exceeding the mean within the AOI reported for 2015-2016 (2.91 m/year) based on UAV photogrammetry [9], and for 2014-2015 (3.28 m/year), which represents the maximum mean displacement 1954-2017 but was derived with terrestrial RTK-GNSS scaled to the AOI [9]. At the same site, the maximum 2023-2024 value (4.66 m/year) also exceeded the 2015-2016 maximum (3.56 m/year) [9], highlighting a clear acceleration at TRG.

At LRG, velocities were more variable. The maximum 2023 2024 velocity was 6.19 m/year (7.08 m/year for the LRG_003m_512 parameterization), higher than the 5.76 m/year reported by Kaufman et al. [10] for 2019-2020. However, the sector where the 2019 2020 maximum occurred exhibited substantially lower values in 2023 2024 (4.4 m/year to 4.8 m/year). In general, the main body of LRG was characterized by lower velocities (<5 m/year), whereas the this zone contained extensive areas exceeding 5 m/year in 2019 2020 [10]. In contrast, our 2023 2024 data show markedly higher velocities in the frontal zone, indicating a contemporaneous acceleration at the front and deceleration in the central sections.

The accuracy assessment and LoD indicate robust velocity computation over all sites and for all UAV campaigns. Values between 0.03 and 0.07 are at the lower end compared to previously published results on high-resolution RG velocities [7], although direct comparisons have to be interpreted with caution due to different settings and study designs. However, comparing LoD and errors of photogrammetric processing in the cm range to annual displacements at the m-scale support robustly computed velocity rates.

The general acceleration observed at TRG in 2023 2024, representing the highest published, photogrammetrically derived RGVs at this site, coincided with the highest air and ground temperatures recorded by sensors installed directly on the RG. At Sonnblick station (~21 km away from TRG), the annual all-time temperature record (in terms of MAAT) since 1887 was reported for 2024, emphasizing the broader regional warming signal. These findings support the established link between increased RGVs and elevated permafrost temperatures [2,4], and suggest a continuation of rising displacement rates consistent with the parallel warming trend and record temperatures at TRG. Additionally, an above-average snowpack during winter 2023 2024 may have contributed to higher velocities through enhanced insulation from winter cold and/or increased water input following melt [2]. It is noteworthy that unpublished point-based RTK-GNSS observations at both sites indicate that the temporal peak in RGV may have occurred during 2020–2021, followed by a decline [28,29]. Nevertheless, the 2023 2024 RGVs at both TRG and LRG rank among the highest when compared to published photogrammetric datasets.

Compared to TRG, LRG presents a more complex coupling between climate and kinematics in this study. While Sonnblick station data show record-breaking mean annual temperatures, local MAGST and snow cover at LRG were not exceptional in 2023 2024 relative to conditions between 2018 and 2024. Furthermore, spatially heterogeneous velocity patterns persist, with acceleration concentrated at the frontal zone and deceleration evident in central parts. This pattern likely reflects not only climatic and hydrological influences but also intrinsic kinematic evolution described by Kaufmann et al. [10], with acceleration of the central zone since 2009 that has propagated westward and is now showing in increased frontal velocities, contributing to the maxima observed

in our study. Consequently, although significant climate-RGV correlations were reported for LRG [10], the relationship appears non-linear and mediated by internal RG dynamics. Longer, spatially resolved kinematic time series combined with comprehensive local climate monitoring will be necessary to disentangle these interactions.
Overall, our findings highlight ongoing changes in permafrost dynamics under accelerating warming in high mountain environments. The strong acceleration at TRG aligns with regional records of air temperature and local ground warming, while LRG illustrates how internal deformation patterns can modulate, delay, or redistribute the climatic signal across a RG. These results emphasize the need for multi-sensor, multi-scale monitoring to capture both climatic forcing and internal kinematic processes that govern RGV variability.

REFERENCES

[1] L. Schrott, R. Bell, & J. H. Blöthe, "Mountain hazards and permafrost degradation," in *Safeguarding Mountain Social-Ecological Systems*, Elsevier, 2024, pp. 31–41. doi: 10.1016/B978-0-12-822095-5.00005-X.

[2] Y. Hu *et al.*, "Rock Glacier Velocity: An Essential Climate Variable Quantity for Permafrost," *Reviews of Geophysics*, vol. 63, no. 1, p. e2024RG000847, 2025, doi: 10.1029/2024RG000847.

[3] S. Piccinelli & N. Cannone, "Divergent Responses of Alpine Rock Glaciers to Climate Change: A Review of Ecological and Abiotic Dynamics," *Permafrost and Periglacial Processes*, vol. 36, no. 3, pp. 438–450, 2025, doi: 10.1002/ppp.2278.

[4] A. Kellerer-Pirklbauer *et al.*, "Acceleration and interannual variability of creep rates in mountain permafrost landforms (rock glacier velocities) in the European Alps in 1995–2022," *Environ. Res. Lett.*, vol. 19, no. 3, p. 034022, Feb. 2024, doi: 10.1088/1748-9326/ad25a4.

[5] RGIK, "Rock Glacier Velocity as an associated parameter of ECV Permafrost: Baseline concepts (Version 3.2)," IPA Action Group Rock glacier inventories and kinematics. Accessed: Nov. 27, 2025. [Online]. Available: https://bigweb.unifr.ch/Science/Geosciences/Geomorphology/Pub/Website/IPA/CurrentVersion/Current_RockGlacierVelocity.pdf

[6] H. Zandler, J. Abermann, B. A. Robson, A. Maschler, T. Scheiber, J. L. Carrivick, & J. C. Yde, "Deep learning outperforms existing algorithms in glacier surface velocity estimation with high-resolution data – the example of Austerdalsbreen, Norway," *Front. Remote Sens.*, vol. 6, May 2025, doi: 10.3389/frsen.2025.1586933.

[7] C. Fey & K. Krainer, "Analyses of UAV and GNSS based flow velocity variations of the rock glacier Lazaun (Ötztal Alps, South Tyrol, Italy)," *Geomorphology*, vol. 365, p. 107261, Sep. 2020, doi: 10.1016/j.geomorph.2020.107261.

[8] V. Kaufmann, W. Sulzer, G. Seier, & M. Wecht, "Panta Rhei: Movement Change of Tschadinhorn Rock Glacier (Hohe Tauern Range, Austria), 1954–2017 https://doi.org/10.32909/kg.18.31.1," *Kartografija i geoinformacije (Cartography and Geoinformation)*, vol. 18, no. 31, Art. no. 31, Apr. 2019, Accessed: Oct. 17, 2024. [Online]. Available: http://kig.kartografija.hr/index.php/kig/article/view/854

[9] V. Kaufmann, G. Seier, W. Sulzer, M. Wecht, Q. Liu, G. Lauk, & M. Maurer, "Rock glacier monitoring using aerial photographs: conventional vs. UAV-based mapping - a comparative study," *Int. Arch. Photogramm. Remote Sens. Spatial Inf. Sci.*, vol. XLII–1, pp. 239–246, Sep. 2018, doi: 10.5194/isprs-archives-XLII-1-239-2018.

[10] V. Kaufmann, A. Kellerer-Pirklbauer, & G. Seier, “Conventional and UAV-Based Aerial Surveys for Long-Term Monitoring (1954–2020) of a Highly Active Rock Glacier in Austria,” *Front. Remote Sens.*, vol. 2, Oct. 2021, doi: 10.3389/frsen.2021.732744.

[11] Land Kärnten, “Digitales 10m - Geländemodell aus Airborne Laserscan Daten der Österreichischen Länder.” Accessed: Jan. 15, 2025. [Online]. Available: https://www.data.gv.at/katalog/en/dataset/land-ktn_digitales-gelandemodell-dgm-osterreich#resources

[12] Emlid, “Emlid Studio,” Emlid. Accessed: Jan. 16, 2026. [Online]. Available: https://docs.emlid.com/emlid-studio/

[13] Emlid, “Reach RS3,” Emlid. Accessed: Jan. 22, 2025. [Online]. Available: https://emlid.com/reachrs3/

[14] Agisoft, “Agisoft Metashape Professional V 2.3.” [Online]. Available: https://www.agisoft.com/downloads

[15] S. Aati, C. Milliner, & J.-P. Avouac, “A new approach for 2-D and 3-D precise measurements of ground deformation from optimized registration and correlation of optical images and ICA-based filtering of image geometry artifacts,” *Remote Sensing of Environment*, vol. 277, p. 113038, Aug. 2022, doi: 10.1016/j.rse.2022.113038.

[16] S. Aati, *Geospatial-COSICorr3D GitHub page*. (Dec. 31, 2024). Python. Accessed: Jan. 16, 2025. [Online]. Available: https://github.com/SaifAati/Geospatial-COSICorr3D

[17] S. Leprince, S. Barbot, F. Ayoub, & J.-P. Avouac, “Automatic and Precise Orthorectification, Coregistration, and Subpixel Correlation of Satellite Images, Application to Ground Deformation Measurements,” *IEEE Transactions on Geoscience and Remote Sensing*, vol. 45, no. 6, pp. 1529–1558, Jun. 2007, doi: 10.1109/TGRS.2006.888937.

[18] S. D. Jawak, S. Kumar, A. J. Luis, M. Bartanwala, S. Tummala, & A. C. Pandey, “Evaluation of Geospatial Tools for Generating Accurate Glacier Velocity Maps from Optical Remote Sensing Data,” in *The 2nd International Electronic Conference on Remote Sensing*, MDPI, Mar. 2018, p. 341. doi: 10.3390/ecrs-2-05154.

[19] H. Zandler, W. Sulzer, & V. Kaufmann, “Delineation of debris-covered glaciers with multi-temporal UAV images (Gössnitzkees, Schober Group/Austria),” *Advances in Geodesy and Geoinformation*, vol. 74, no. 1, pp. e66, 1–17, Jun. 2025, doi: 10.24425/agg.2025.154150.

[20] P. Kraaijenbrink, S. W. Meijer, J. M. Shea, F. Pellicciotti, S. M. De Jong, & W. W. Immerzeel, “Seasonal surface velocities of a Himalayan glacier derived by automated correlation of unmanned aerial vehicle imagery,” *Ann. Glaciol.*, vol. 57, no. 71, pp. 103–113, Jan. 2016, doi: 10.3189/2016AoG71A072.

[21] F. Paul *et al.*, “Error sources and guidelines for quality assessment of glacier area, elevation change, and velocity products derived from satellite data in the Glaciers_cci project,” *Remote Sensing of Environment*, vol. 203, pp. 256–275, Dec. 2017, doi: 10.1016/j.rse.2017.08.038.

[22] B. Staub, A. Hasler, J. Noetzli, & R. Delaloye, “Gap-Filling Algorithm for Ground Surface Temperature Data Measured in Permafrost and Periglacial Environments: Gap-Filling Algorithm for GST Data Measured in Permafrost Environments,” *Permafrost and Periglac. Process.*, vol. 28, no. 1, pp. 275–285, Jan. 2017, doi: 10.1002/ppp.1913.

[23] I. Auer *et al.*, “HISTALP—historical instrumental climatological surface time series of the Greater Alpine Region,” *Intl Journal of Climatology*, vol. 27, no. 1, pp. 17–46, Jan. 2007, doi: 10.1002/joc.1377.

[24] S. S. David A Swayne & C. Obimbo, “Automating the Smoothing of Time Series Data,” *J Environ Anal Toxicol*, vol. 05, no. 05, 2015, doi: 10.4172/2161-0525.1000304.

[25] L. Cheng, G. Foster, Z. Hausfather, K. E. Trenberth, & J. Abraham, “Improved Quantification of the Rate of Ocean Warming,” *Journal of Climate*, vol. 35, no. 14, pp. 4827–4840, Jul. 2022, doi: 10.1175/JCLI-D-21-0895.1.

[26] S. A. Khan, H. Zandler, & O. Sass, “Climate change impacts on livelihoods in the Eastern Hindu Kush: integrating local perceptions and biophysical data,” *Reg Environ Change*, vol. 25, no. 3, p. 114, Sep. 2025, doi: 10.1007/s10113-025-02414-9.

[27] I. Haag, P. D. Jones, & C. Samimi, “Central Asia’s Changing Climate: How Temperature and Precipitation Have Changed across Time, Space, and Altitude,” *Climate*, vol. 7, no. 10, Art. no. 10, Oct. 2019, doi: 10.3390/cli7100123.

[28] V. Kaufmann, “Website for access to geodetic measurement results of Leibnitzkopf rock glacier.” 2025. [Online]. Available: https://www.staff.tugraz.at/viktor.kaufmann/Leibnitzkopf_Rock_Glacier/index.html

[29] V. Kaufmann, “Website for access to geodetic measurement results of Tschadinhorn rock glacier.” 2025. [Online]. Available: https://www.staff.tugraz.at/viktor.kaufmann/Tschadinhorn_Rock_Glacier/index.html